Ocean Acoustic Propagation: Fluctuations and Coherence in Dynamically Active Shallow-Water Regions

Timothy F. Duda
Applied Ocean Physics and Engineering Department, MS 11
Woods Hole Oceanographic Institution, Woods Hole, MA 02543
phone: (508) 289-2495 fax: (508) 457-2194 email: tduda@whoi.edu

Grant Number: N00014-05-1-0482
http://www.whoi.edu/science/AOPE/cofdl/timdcv.html

LONG TERM GOALS

The goals are to understand the nature and causes of acoustic signal fluctuations in the shallow water environment (i.e. the physical mechanisms). This may enhance prediction of acoustic system performance and enable exploitation of oceanographic variability and signal features. Here, signal means any identifiable acoustic reception, including sounds of unknown origin, identifiable signals from discrete sources, and intentional signals.

OBJECTIVES

An objective is to gain understanding of the fluctuation behavior of fully three-dimensional acoustical propagation (including horizontal deflection from seafloor and water column heterogeneities) in shallow-water environments with three-dimensional structure at all significant scales. This will allow evaluation of commonly used two-dimensional approximations for ocean structures and propagation physics. A second objective is to classify acoustic stability and fluctuation using signal parameters. We are also investigating the time scales over which the often-invoked assumption of stationary conditions is valid.

APPROACH

To understand and predict shallow-water acoustic conditions, including examination of the influences of three-dimensional shallow-water oceanic features on propagation, we have been analyzing experimental data and implementing propagation modeling and theory. The effort is aimed primarily at summer conditions in the temperate ocean (an approximate two-layer system), but also includes conditions found just inshore of shelfbreak fronts. An example is the front such in the Mid-Atlantic Bight where there is warm water offshore and winter-cooled water on the shelf. In this particular frontal zone there can be a thin deep warm salty layer, capped by an inverse thermocline, on the near-edge section of the shelf. Internal tides and nonlinear mode-one internal gravity waves are known to often dominate in these regimes. The acoustic effects of these waves are the main subjects of our research. Such waves at the location of a sound source would control acoustic mode excitation, and thus the effects of mode-stripping on long propagation paths. Such waves along a sound propagation path can cause mode coupling, altering mode-stripping effects at further range, and mode refraction.

Report Documentation Page

Form Approved
OMB No. 0704-0188

1. REPORT DATE	2. REPORT TYPE	3. DATES COVERED
2009		**00-00-2009 to 00-00-2009**

4. TITLE AND SUBTITLE	5a. CONTRACT NUMBER
Ocean Acoustic Propagation: Fluctuations And Coherence In Dynamically Active Shallow-Water Regions	5b. GRANT NUMBER
	5c. PROGRAM ELEMENT NUMBER
6. AUTHOR(S)	5d. PROJECT NUMBER
	5e. TASK NUMBER
	5f. WORK UNIT NUMBER
7. PERFORMING ORGANIZATION NAME(S) AND ADDRESS(ES) **Woods Hole Oceanographic Institution,Applied Ocean Physics and Engineering Department, MS 11,Woods Hole,MA,02543**	8. PERFORMING ORGANIZATION REPORT NUMBER
9. SPONSORING/MONITORING AGENCY NAME(S) AND ADDRESS(ES)	10. SPONSOR/MONITOR'S ACRONYM(S)
	11. SPONSOR/MONITOR'S REPORT NUMBER(S)

12. DISTRIBUTION/AVAILABILITY STATEMENT
Approved for public release; distribution unlimited

13. SUPPLEMENTARY NOTES

14. ABSTRACT
The goals are to understand the nature and causes of acoustic signal fluctuations in the shallow water environment (i.e. the physical mechanisms). This may enhance prediction of acoustic system performance and enable exploitation of oceanographic variability and signal features. Here, signal means any identifiable acoustic reception, including sounds of unknown origin, identifiable signals from discrete sources, and intentional signals.

15. SUBJECT TERMS

16. SECURITY CLASSIFICATION OF:			17. LIMITATION OF ABSTRACT	18. NUMBER OF PAGES	19a. NAME OF RESPONSIBLE PERSON
a. REPORT	b. ABSTRACT	c. THIS PAGE			
unclassified	**unclassified**	**unclassified**	**Same as Report (SAR)**	**11**	

Long internal waves or internal tides (having wavelengths tens of kilometers) can alter mode shapes and mode stripping, and can alter source excitation, but probably do not cause mode coupling.

We are comparing our theoretically based ideas and computationally derived results with ground-truth field observations from four experiments. One is the ONR ASIAEX South China Sea study. This study yielded four papers in the October 2004 *IEEE Journal of Oceanic Engineering* containing analysis of acoustic signals at 250-450 Hz from sources at ranges of 21 and 32 kilometers: Orr et al. [2004], Mignerey and Orr [2004], Chiu *et al*. [2004], and Duda *et al*. [2004]. The next experiment is the Littoral Environmental Acoustics Research (LEAR) portion of the ONR Shallow-Water 2006 experiment (SW06). This experiment was on the shelf in the Mid-Atlantic Bight east of New Jersey, and took place July-September 2006 [Tang *et al*., 2007]. The third experiment is the spring 2007 ONR/Taiwan NLIWI acoustics experiment in the ASIAEX area of the South China Sea [Reeder *et al*., 2008]. The fourth is the ONR Quantifying, Predicting and Exploiting Uncertainty experiment (QPE), with major observations made in the East China Sea in Sept. 2009.

To better investigate horizontal refraction we have moved into 3-D parabolic equation (PE) computational acoustic modeling. This tool is essential in sloped environments and where high lateral sound-speed gradients are found (such as in nonlinear internal waves, where the modal refractive index has been observed to vary up to one-half percent, and acoustic mode critical angles can exceed five degrees [Reeder *et al*., 2008]).

The goal of the classification work is to identify unique shallow-water fluctuation regimes, classified in terms of fluctuation parameter state vectors received by an array, and relate them to their causes (large internal waves, small internal waves, focusing by alignment with internal wave crests, etc.). The ability to classify the propagation domain (i.e. identify the cause of dominating fluctuations) would enable modeling, prediction, and extrapolation. If received data alone could be used to identify the fluctuation regime, this would be a through-the-sensor technique.

WORK COMPLETED

A large number of LEAR/SW06 pulses transmitted from moored sources to the WHOI L-array (co-located HLA/VLA) have been analyzed. Figure 1 shows the experimental arrangement. Figures 2 and 3 show coherence length estimates and other parameters obtained from analysis of HLA signals after array shape correction and beam steering. The figures show that the sound arrival angle is altered and coherence length is diminished by the presence of internal waves between the source and receiver. The coherence length at fixed steering angle fluctuates greatly because of sound refraction and waveform interference. The time series of maximum observed coherence length is slightly more regular and reaches very long lengths because refraction is adaptively corrected for, but the maximum coherence length is not always long, with low values at times of wave activity. The coherence function of the complex field is governed by phase fluctuations along the length of the array, with amplitude fluctuations taking a secondary role. The processing method is effectively broadband because entire pulse arrival time series at each phone are correlated against each other to achieve the result.

Figure 4 shows an interpretation of the results. The curves show hypothetical coherence versus beam steering angle from broadside, which would require a larger experiment to measure. (We only have simultaneous measurements at two angles, 28 and 300 degrees.) Many pulses are required to effectively measure the coherence angle, and the time series is crucial for interpreting the causes of the behavior, so analysis of intermittent towed-source pulses transmitted to the L-array from other

directions by other SW06 PI's would not be helpful in building up the full curves. A manuscript describing the one-month time series of observations along the two paths is in progress, building on our published paper [Collis *et al*., 2008].

This year, our Cartesian coordinate 3-D parabolic equation (PE) code has been used extensively. Added this year is a better wide-angle starter. Also, the coding has been changed to allow layers to have differing density, with density still needing to be uniform in subdomains (i.e. vertical layers) but density interfaces now allowed. This work is done in collaboration with Y.-T. Lin of WHOI.

A paper that used the code was published showing how an internal wave duct that fades into the background state can emit highly variable beams of sound (Lin *et al.*, 2009). At frequencies of a few hundred hertz, each acoustic mode has its own structure, evolving in time as the wave or sound source moves, so that receivers past the end of the duct see rapid variations of mode content and of overall sound level. A second paper was submitted on the topic of sound in curved internal waves, with Lynch as first author, which included 3-D PE modeling of sound through realistic internal waves. Further modeling was applied to the 2007 South China Sea experiment. Figure 5 shows the experiment region. The conditions measured by the 2007 South China Sea PI's were used to model sound propagation. Initial results show promising agreement with measurements [Reeder *et al.*, 2008]. The simulations mimic the propagation (essentially) along the curved waves, which is what was measured (the experimental geometry was chosen for this purpose). The simulations provide results at many angles besides those measured in the field, so other effects may be discovered.

Finally, data have recently been obtained from QPE PI's. Some of the internal waves and large internal tides measures in the program are shown in Figure 6. The predicted and observed acoustic propagation effects in this area will be compared against those tabulated in the earlier studies mentioned above.

RESULTS

Sound refraction effects measured at the South China Sea site were found to be consistent with model results. Initial results were published in an Oceans meeting paper [Reeder *et al*., 2008]. The paper reports mode refractive indices and critical angles of the internal waves present during the experiment. The 3D acoustic effects were replicated with propagation through straight internal waves using the 3-D propagation code. The good comparison between the experiment and the initial model output suggests that behavior at source-receiver geometries other than that of the experiment (down the internal wave duct, Figure 5) can be examined. This year, propagation through curved internal waves more consistent with the observations showed very similar results, with the addition of a new effect: surface ducting at different azimuth angles than low-mode deep ducting. In the curved-wave situation, critical mode refraction effects evolve as the sound moves along the curved duct, rather than being constant. As a result, the internal waves may behave like prisms, separating modes.

As mentioned in the previous section, an examination of propagation down an internal wave duct that fades away, as was observed a few times in SW06, was performed in collaboration with Y.-T. Lin of WHOI. This is due to be published in late 2009. The results show that a highly time-dependent mix of acoustic mode beams can emerge from the duct, with the beams of each mode appearing to be independent.

Time series of internal tides and nonlinear internal wave packets were measured at many SW06 moorings. These each propagate (often in the same direction) at speeds of 0.7 to 0.8 m/s. The internal

tides have wavelength of 25 to 40 km, whereas the nonlinear waves have 300 to 1200 m wavelengths. Using the time series to construct a realistic temporally evolving vertical slice of sound speed (similar to Chui *et al*. 2004), time-varying signal level vs. range curves can be generated. At 9 km range, depth-averaged signals can vary by 6 dB (depth averaging quantifies seafloor loss effects), with range-averaged single-depth arrivals being even more variable. The effects of varying mode excitation by the fixed-depth source, as well as that of varying mode attenuation parameters, are being examined for relative importance.

Finally, a further analysis of the SW06 fluctuation data set that was partially analyzed and published [Collis *et al.*, 2008] puts the preliminary results into context. The highly variable horizontal array gain and coherence length variability for along-internal wave duct propagation in SW06 is now tabulated for the entire experiment. Results for the across-internal wave path have also been computed, which are much less variable in time. The manuscript is in preparation.

IMPACT/APPLICATIONS

The results may be useful in the signal processing domain. Algorithms may be developed that are robust to signal fluctuations, or which may exploit them. For example, processing might exploit fluctuations by utilizing intermittent but strong signal peaks, or predicting time limits for coherent analysis, or predicting wait-time intervals before signals are reacquired after fade-outs.

RELATED PROJECTS

For the LEAR portion of SW06, the PI is working with Drs. J. Collis (Colorado School of Mines), H. DeFerrari (Miami), J. Lynch (WHOI) M. Badiey (U Del.), and J. Nash (OSU). The PI collaborates with Dr. Y.-T. Lin of WHOI on computational efforts. The PI is working with ONR PI's analyzing data from the SW06, 2007 South China Sea, and QPE experiment sites, and participated in one QPE cruise in Sept, 2009. Ilya Udovydchenkov is supervised by the PI as an ONR postdoctoral fellow, and is working on coupled-mode long-distance deep-water acoustics.

REFERENCES

Chiu, C.-S., S. R. Ramp, C. W. Miller, J. F. Lynch, T. F. Duda, and T. Y. Tang, Acoustic intensity fluctuations induced by South China Sea internal tides and solitons, *IEEE J. Oceanic Eng., 29*, 1249-1263, 2004.

Duda, T. F., J. F. Lynch, A. E. Newhall, L. Wu, and C.-S. Chiu, Fluctuation of 400-Hz sound intensity in the 2001 ASIAEX South China Sea Experiment, *IEEE J. Oceanic Eng., 29*, 1264-1279, 2004.

Mignerey, P. C. and M. H. Orr, Observations of matched-field autocorrelation time in the South China Sea, *IEEE J. Oceanic. Eng., 29*, 1280-1291, 2004.

Orr, M. H., B. H. Pasewark, S. N. Wolf, J. F. Lynch, T. Schroeder, and C. -S. Chiu, South China Sea internal tide/internal waves - Impact on the temporal variability of horizontal array gain at 276 Hz, *IEEE J. Oceanic. Eng., 29*, 1292-1307, 2004.

PUBLICATIONS

Heaney, K. D., G. Gawarkiewicz, T. F. Duda and P. F. J. Lermusiaux, Non-linear optimization of autonomous undersea vehicle sampling strategies for oceanographic data assimilation, *J. Field Robotics, 24,* 437-448, 2007. [published, refereed]

Newhall, A. E., T. F. Duda, K von der Heydt, J. D. Irish, J. N. Kemp. S. A. Lerner, S. P. Liberatore, Y.-T. Lin, J. F. Lynch, A. R. Maffei, A. K. Morozov, A. Shmelev, C. J. Sellers, W. E. Witzell, Acoustic and oceanographic observations and configuration information for the WHOI moorings from the SW06 experiment, *Woods Hole Oceanog. Inst. Tech. Rept.*, WHOI-2007-04, June 2007. [published, not refereed]

Duda, T. F., B. M. Howe and J. H. Miller, Acoustics in global process ocean observatories, *Sea Technology, 48,* 35-38, 2007. [published, not refereed]

Duda, T. F., Examining the validity of approximations to fully three-dimensional shallow-water acoustic propagation through nonlinear internal gravity waves, *IEEE Oceans '07 Aberdeen Conference proceedings,* June 2007. [published, not refereed]

Duda, T. F. and J. Collis, Acoustic field coherence in four-dimensionally variable shallow-water environments: estimation using co-located horizontal and vertical line arrays, *Underwater Acoustic Measurement and Technology Conference Proceedings,* Crete, Greece, June 2007. (Invited paper) [published, not refereed]

Irish, J. D., J. F. Lynch, J. N. Kemp, T. F. Duda, and A. E. Newhall, Moored array for measuring internal solitary waves during Shallow Water 06, *MTS/IEEE Oceans '07 Vancouver Conference Proceedings,* 2007. [published, not refereed]

Tang, D. J., J.N. Moum, J.F. Lynch, P. Abbot, R. Chapman, P. Dahl, T. Duda, G. Gawarkiewicz, S. Glenn, J.A. Goff, H. Graber, J. Kemp, A. Maffei, J. Nash and A. Newhall, ShallowWater 2006: a joint acoustic propagation/nonlinear internal wave physics experiment, *Oceanography,* 20(4), 156-167, 2007. [published, refereed]

Reeder, D. B., T. F. Duda and B. Ma, Short-range acoustic propagation variability on a shelf area with strong nonlinear internal waves, *IEEE Oceans '08 Kobe Conference Proceedings*, April 2008. [published, not refereed].

Duda, T. F., and L. Rainville, Diurnal and semidiurnal internal tide energy flux at a continental slope in the South China Sea, *J. Geophys Res (C), 113,* C03025, doi:10.1029/2007JC004418, 2008. [published, refereed]

Duda, T. F. and A. D. Pierce, History of Environmental Acoustics, 1960's to 2000's, *MTS/IEEE Oceans '08 Quebec Conference Proceedings,* 2008. Invited paper. [published, not refereed].

Collis, J. M., T. F. Duda, J. F. Lynch, and H. A. Deferrari, Observed limiting cases of horizontal field coherence and array performance in a time-varying internal wavefield, *J. Acoust. Soc. Am., 124,* EL97, 2008. [published, refereed]

Li, Q., D. M. Farmer, T. F. Duda, and S. Ramp, Measurement of nonlinear internal waves using the inverted echo sounder, *J. Atmos Oceanic Technol.,* in press, 2009. [published, refereed]

Lin, Y.-T., T. F. Duda, and J. F. Lynch, Acoustic mode radiation from the termination of a truncated nonlinear internal gravity wave duct in a shallow ocean area, *J. Acoust. Soc. Am.,* in press, 2009. [published, refereed]

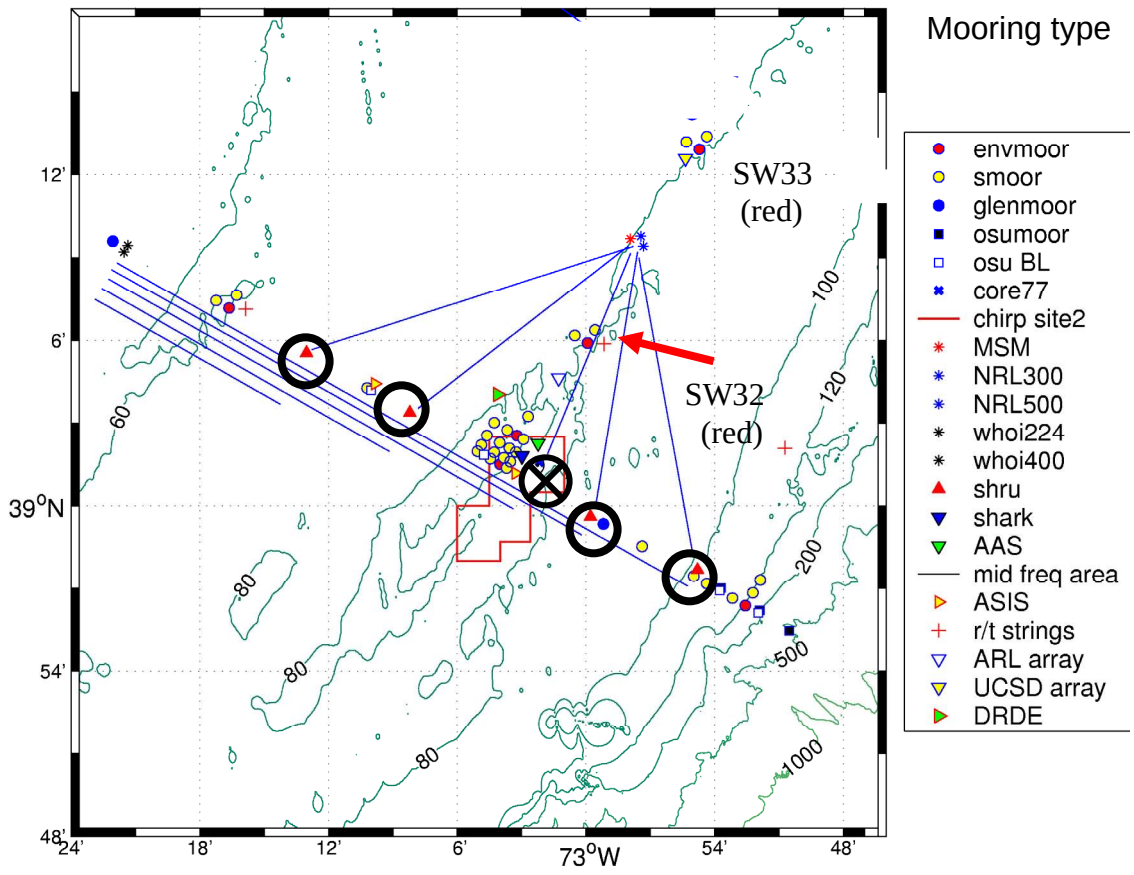

Figure 1. SW06 propagation paths from moored sources to moored receivers are shown with blue lines. The circles show single-phone SHRU receivers. The circle with the X shows the WHOI L-array (vertical line array (VLA) attached to horizontal line array (HLA) on the seafloor). The northwest site had 224 and 400 Hz sources. The northeast site had 100, 200, 300, 400, and 800 Hz sources. Environmental mooring SW32 whose data are shown in Figs. 2 and 3 is marked. Depths are contoured in meters.

[The L-array is near the center. At heading 30 (approx) are SW32 at 10 km distance and the northeast sources at 20 km. The four SHRUS are near a line of heading 300, two offshore of the L-array and two inshore. The northwest sources are 32 km from the L-array along this line at about 60-m depth. The L-array and the 30-degrees line are at about 80-m depth.]

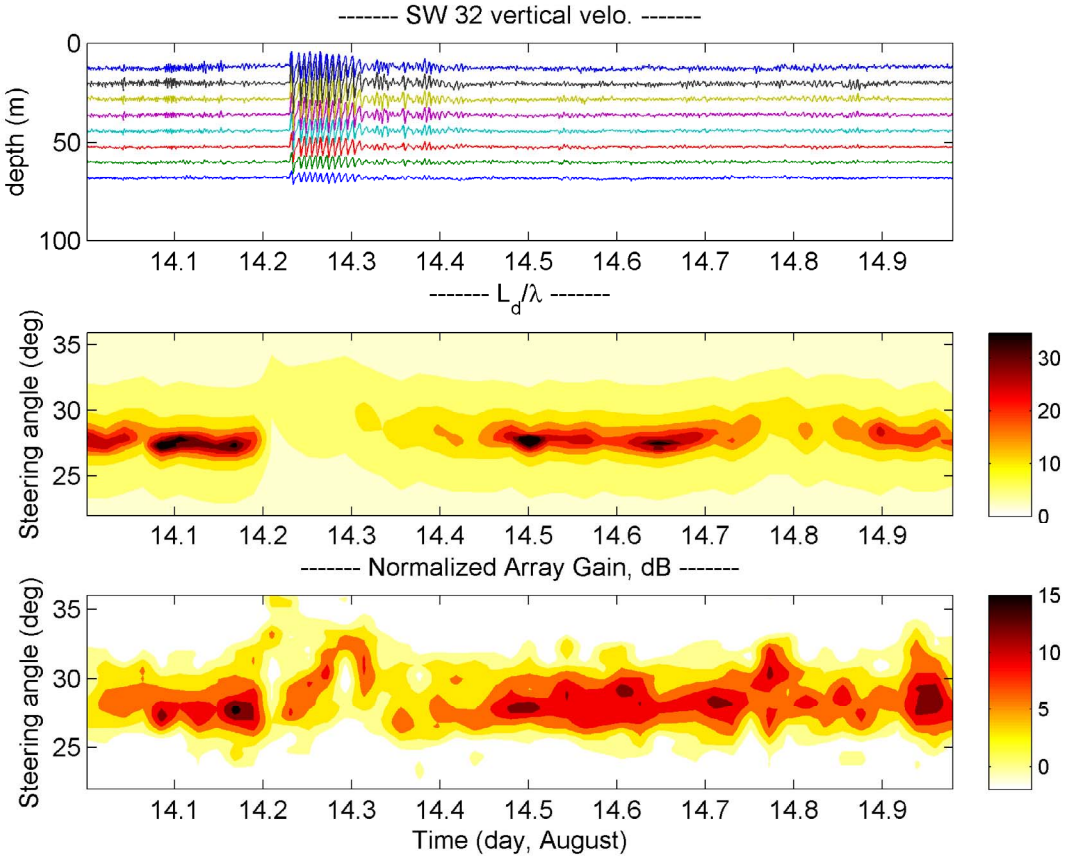

Figure 2. One-day long time series of derived quantities from 200-Hz pulses transmitted from the northeast site are show, along with internal waves measured along the path. (top) Vertical velocity at a few depths at site SW32). Velocity is scaled arbitrarily so that internal waves are visible. Time series for each depth are plotted so that zero value is located at the measurement bin depth. One packet of steep nonlinear waves is seen. (center) Contours of horizontal coherence length, normalized by acoustic wavelength, computed for pulses received along the HLA. Coherence length is computed as a function of time and beam steering angle. The maximum coherence length is reduced when the sound passes through the waves, which are aligned such that sound travels along the crests. (bottom) The coherent-average signal power versus noise power (array gain) for the 32-element HLA is plotted as a function of beam steering angle and time. The sound is diverted by the waves and appears to arrive from a more easterly heading. The theoretical gain for a plane wave signal and incoherent noise is 10log(32) ~ 15 dB. High array gain is intermittently achieved. The angle at which array gain reaches maximum fluctuates. Gain is reduced during the internal wave event.

[(top) 14 large internal waves appear between day August 14.23 and 14.31. (center) The correlation length detected at steering angle 28 degrees is usually 20-30 wavelengths, decreasing from this peak at other angles. At the time of the waves the peak is at about 30 degrees and is reduced to about 5 wavelengths. (bottom) The array gain usually has a peak of 10 to 15 dB at steering angle 28 degrees. At the time of the waves there a two brief periods of peak gain less than 5 dB, occurring at rapidly variable angle.]

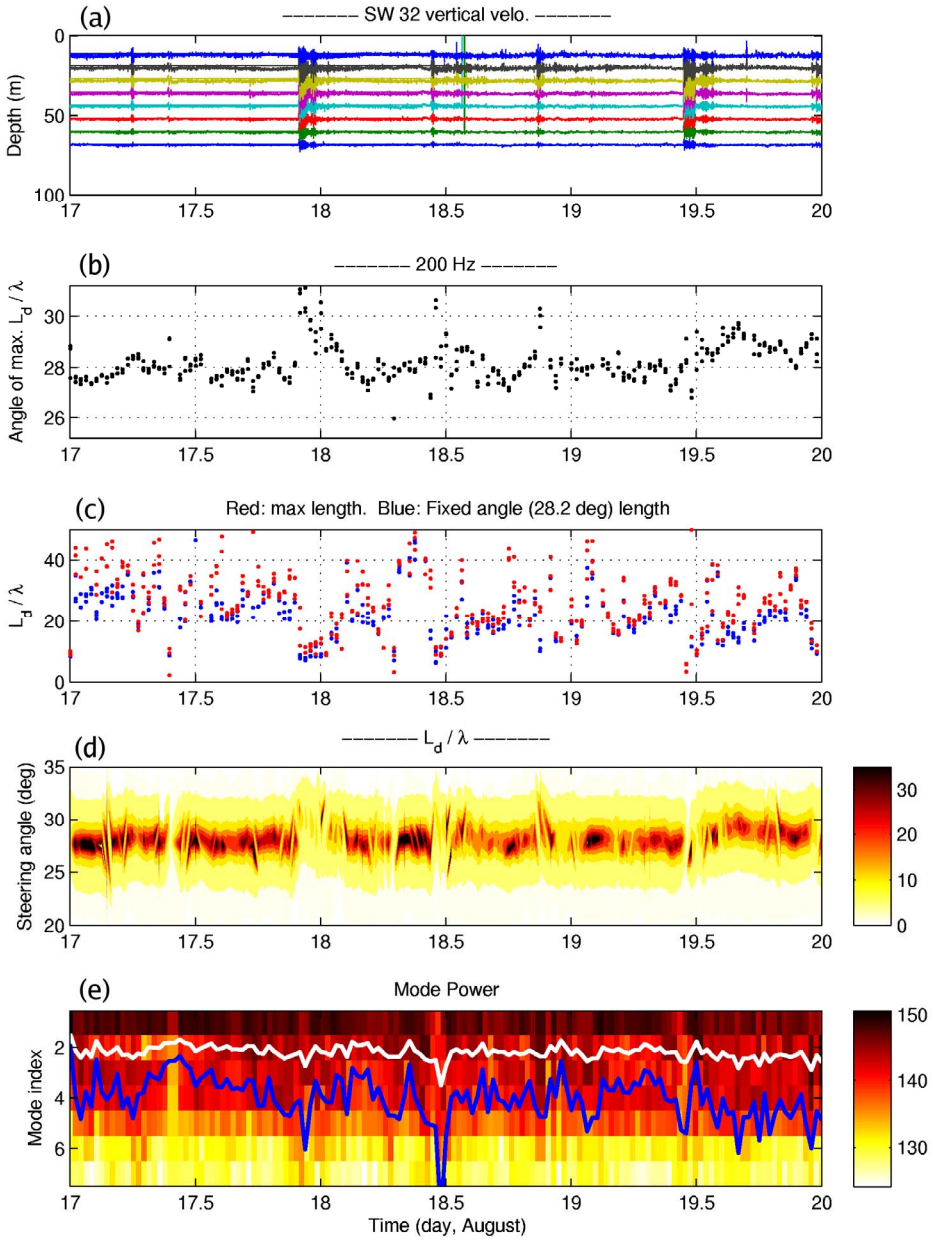

Figure 3. Wave and pulse parameters for the 200-Hz northeast source are shown for August 17-19, 2006. (a) Time series of vertical water velocity along the acoustic path at SW32 show internal wave packets. (b) The HLA steering angle with maximum horizontal field coherence length is shown. (c) The coherence length divided by the acoustic wavelength is plotted. The red dots show the maximum coherence length as a function of time. The blue dots show the coherence length at the fixed angle of 28.2 degrees. (d) The coherence length is contoured versus steering angle and time. [Source of point data shown in (b) and (c)]. The array is moved by the waves at day 19.45, altering the processing bias. (e) Mode content determined from VLA receptions. The blue and white lines show ad hoc measures of mode width. Coupling evidence is seen at some of the times of waves and sound angular deflections.

[During three intervals of strong internal waves the acoustic parameters are altered, with beam angle changing from 28 to 30 degrees and coherence length falling from 40 to 7 wavelengths.]

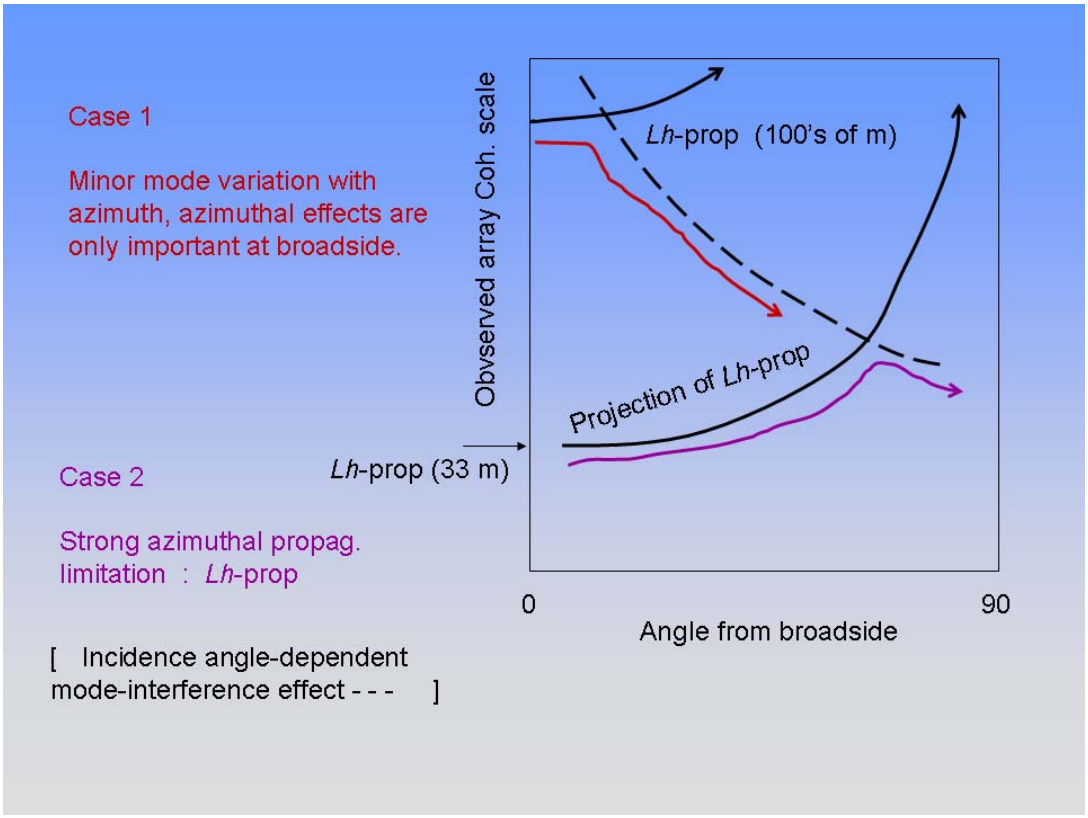

Figure 4. Interpretation of two coherence length situations observed in the 100 and 200-Hz pulse data received at the L-array. The red line (Case 1) corresponds to the long coherence scale case, where interference governs correlation in the experimental situation of 63 degrees from broadside. The lavender line (Case 2) corresponds to the short-coherence scale case, where the coherence at this angle is governed not by ubiquitous mode interference (dashed line), but by decorrelation processes with azimuthal dependence as measured from the source position. Note that the "projection of L_h-propagation" lines rise as $1/\cos\theta$, where θ is angle from broadside.

[As pulse arrival angle from broadside moves from zero to 90 degrees, the red Case-1 line drops. It is near the dashed line for true plane-wave mode arrivals everywhere except at broadside, where it is lower then the dashed line because of weak departure from plane wave geometry (weak azimuthal variability). The lavender Case-2 line starts low at angle zero (broadside) and rises because of a geometric effect until it intersects the dashed line at an angle between 45 and 90 degrees.]

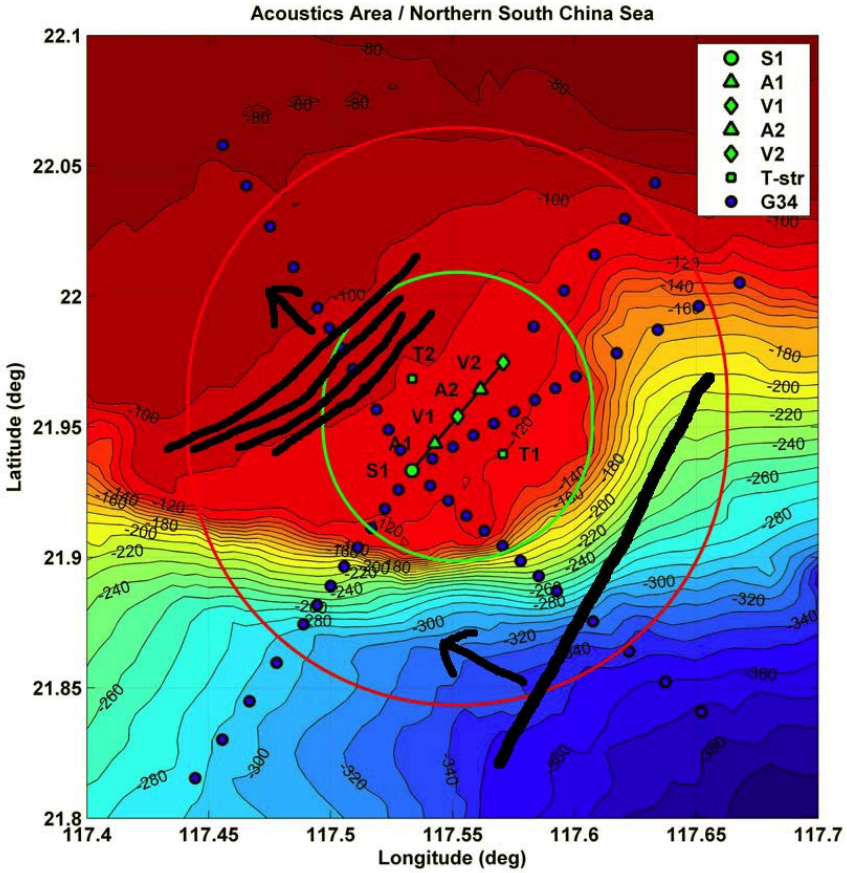

Figure 5. Bathymetric chart showing the 2007 NLIWI experiment area. Eight moorings were placed, shown in green. Five are along the acoustic propagation line: S1, 400-Hz acoustic source; A1 (ADCP) 1.48 km from S1; V1 (VLA) 3.00 km from S1; A2 (ADCP) 4.43 km from S1; and V2 (VLA) 6.01 km from S1. The heading along the mooring line is 40° True. Three additional thermometer array moorings were: T1, 2.45 km @ 130° from V1; T2, 2.50 km @ 310° from V1, and T3, 6.66 km @ 322° from V1. The blue dots show intended dipped acoustic source stations. The black lines schematically depict, at the right, an incident internal wave of depression and at the left a packet of waves on the shelf of the type formed from such waves.

[The A1 to V2 mooring line (acoustic propagation line) is approximately parallel to the crests of nonlinear internal waves arriving from the east.]

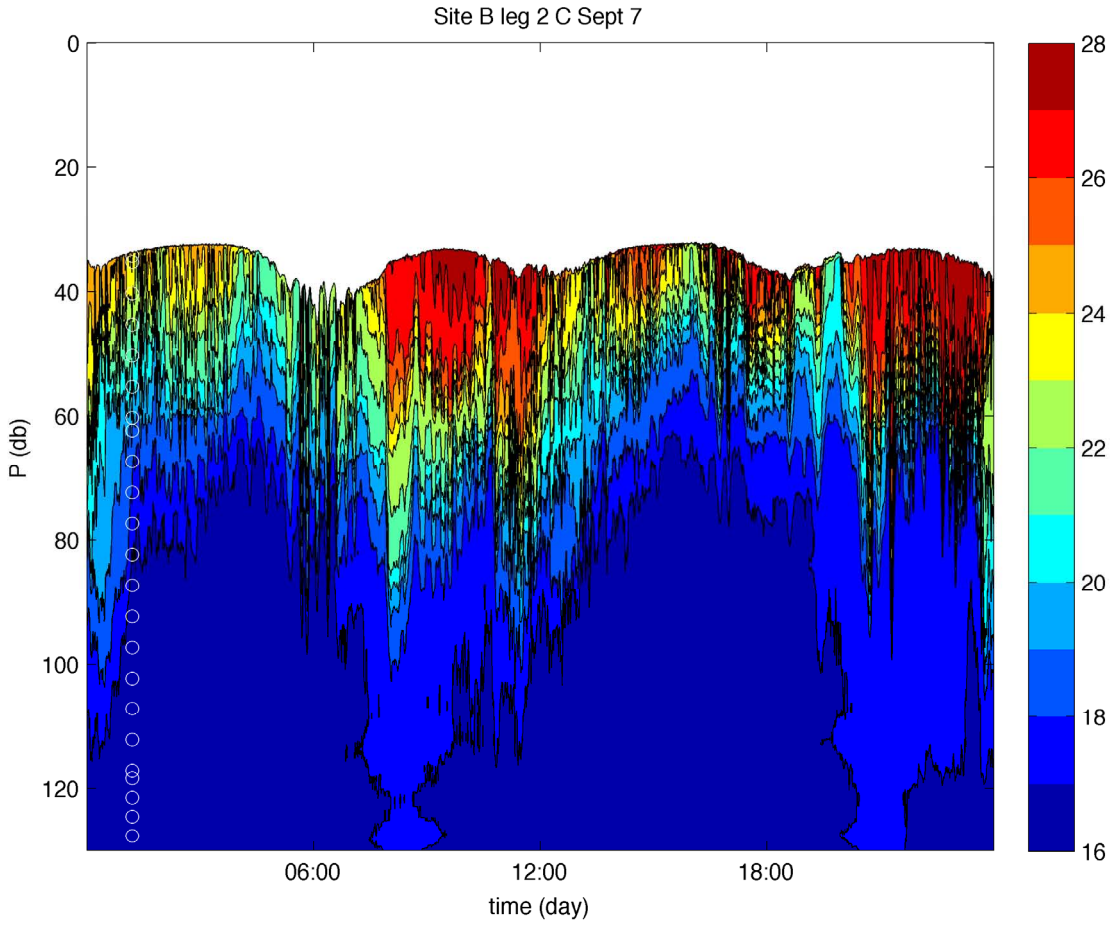

Figure 6. The time-series of temperature profiles measured at a QPE experiment mooring just north of the shelf edge northeast of Taiwan is contoured. A one-day period is shown, 7 Sept. 2009 (UTC time). Temperature is measured at 24 depths between approximately 35 and 135 m depth (140 m seafloor depth), indicated on the left with white circles. The high tidal currents pull down the sensors four times per day; the effect is accounted for in the diagram. Large internal tides are shown, 40-to 50-m in peak-to-peak semidiurnal thermocline displacement. Six or more packets of nonlinear internal waves can also be seen. The large fluctuations in water column structure may induce horizontally anisotropic temporal variability of acoustic propagation conditions.

[Temperature contours from 17 to 27 degrees C are shown. X-Y axes are pressure, 0-130 dbar, and time, 0000-2359 Sept 7. Warm surface waters above 24 C move from above the sensors (not measured) to depths of 70 m from 0800 to 1200 and again at 2000 to 2330. Large short-period nonlinear internal waves appear with these two internal tide displacements, and also appear near 0200, 0600, 1400, and 1700.]